

Meteorological Factors Responsible for Major Power Outages during a Severe Freezing Rain Storm over Eastern Canada

JULIE M. THÉRIAULT,^a VANESSA MCFADDEN,^a HADLEIGH D. THOMPSON,^a AND MÉLISSA CHOLETTE^b

^a *Centre pour l'Étude et la Simulation du Climat à l'Échelle Régionale, Department of Earth and Atmospheric Sciences, Université du Québec à Montréal, Montreal, Quebec, Canada*

^b *Meteorological Research Division, Environment and Climate Change Canada, Dorval, Quebec, Canada*

(Manuscript received 17 October 2021, in final form 28 April 2022)

ABSTRACT: Winter precipitation is the source of many inconveniences in many regions of North America, for both infrastructure and the economy. The ice storm that hit the Canadian Maritime Provinces on 24–26 January 2017 remains one of the most expensive in history for the province of New Brunswick. Up to 50 mm of freezing rain caused power outages across the province, depriving up to one-third of New Brunswick residences of electricity, with some outages lasting 2 weeks. This study aims to use high-resolution atmospheric modeling to investigate the meteorological conditions during this severe storm and their contribution to major power outages. The persistence of a deep warm layer aloft, coupled with the slow movement of the associated low pressure system, contributed to widespread ice accumulation. When combined with the strong winds observed, extensive damage to electricity networks was inevitable. A 2-m temperature cold bias was identified between the simulation and the observations, in particular during periods of freezing rain. In the northern part of New Brunswick, cold-air advection helped keep temperatures below 0°C, while in southern regions, the 2-m temperature increased rapidly to slightly above 0°C because of radiational heating. The knowledge gained in this study on the processes associated with either maintaining or stopping freezing rain will enhance the ability to forecast and, in turn, to mitigate the hazards associated with those extreme events.

SIGNIFICANCE STATEMENT: A slow-moving low pressure system produced up to 50 mm of freezing rain for 31 h along the east coast of New Brunswick, Canada, on 24–26 January 2017, causing unprecedented power outages. Warm-air advection aloft, along with a combination of higher wind speeds and large amounts of ice accumulation, created ideal conditions for severe freezing rain. The storm began with freezing rain along the entire north–south cross section of eastern New Brunswick and changed to rain only in the south, when local temperatures increased to >0°C. Near-surface cold-air advection kept temperatures below 0°C in the north. Warming from the latent heat produced by freezing contributed to persistent near-0°C conditions during freezing rain.

KEYWORDS: Extreme events; Freezing precipitation; Latent heating/cooling; Numerical analysis/modeling

1. Introduction

In recent decades, Canada has experienced many extreme precipitation events, including the 1997 Red River floods (Rannie 2016), the 1998 ice storm in Ontario and Quebec (e.g., Milton and Bourque 1999; Gyakum and Roebber 2001; Roebber and Gyakum 2003), and the 2013 Calgary, Alberta, floods (i.e., Milrad et al. 2015; Pomeroy et al. 2016). Freezing rain and wet snow, and the resulting ice buildup on surfaces and structures (Fig. 1), are among the most complex winter precipitation types to forecast (Ralph et al. 2005; Barszcz et al. 2018) and the most damaging to infrastructure (Szeto et al. 1999; Changnon 2003; Dore 2003).

Considering the severe consequences associated with ice accumulation on structures, several studies have quantified and assessed the occurrence of freezing rain. According to Cortinas et al. (2004), freezing rain occurs frequently in New Brunswick

(NB), Canada, with a median annual duration between 20 and 30 h for the period of 1976–1990. More recently, based on hourly observations over a longer time period, Groisman et al. (2016) reported an average number of days of freezing rain in NB, ranging from 6 to 8 days (144–192 h) per year between 1975 and 2014.

Freezing rain events can pose significant risks due to ice accretion on electrical transmission lines and communication towers (Yip 1995; Stuart and Isaac 1999; Lu and Kielocho 2005; Makkonen et al. 2014; Panteli and Mancarella 2015; Rezaei et al. 2016). Yip (1995) mapped the 30-yr return period for the equivalent radial thickness of ice on a 25-mm diameter wire over Canada. They concluded that, as a result of more frequent freezing rain (Cortinas et al. 2004), the power network in eastern Canada would be more affected than in western Canada, with icing amounts exceeding 30 mm in some areas. In particular, the amount of icing in NB would be highest in the southeast, near Moncton (Lamraoui et al. 2013; Chartrand 2020).

Although research on the climatology of winter precipitation types over the east coast of Canada exists (e.g., Stuart and Isaac 1999; Groleau et al. 2007; Cheng et al. 2011; Ressler et al. 2012), there are few case studies on the meteorological

 Denotes content that is immediately available upon publication as open access.

Corresponding author: Julie M. Thériault, theriault.julie@uqam.ca



FIG. 1. Ice buildup on (a) power lines and (b) tree branches during the 2017 January ice storm over northeastern New Brunswick, near Bas Caraquet (see Fig. 2, below). The photographs were provided by NB Power.

conditions that lead to freezing rain events. Nonetheless, freezing rain events were studied as part of the Canadian Atlantic Storms Program (CASP I and II) in Nova Scotia and Newfoundland, Canada (Stewart 1991). These extreme events can occur in less populated area of North America, such as the province of NB. On 24–26 January 2017, an extreme freezing rain event impacted the Canadian Maritime Provinces (Fig. 2). Ice buildup on trees and power lines (Fig. 1) during the storm resulted in widespread power outages that affected up to 133 000 homes. Power outages lasted up to 2 weeks in some coastal regions. According to NB Power (Wagner 2017), this event was the largest recovery operation in provincial history. Whereas the extreme

1998 ice storm produced 70–110 mm of freezing rain over southern Quebec in almost 96 h, the 24–26 January 2017 ice storm in NB produced up to 50 mm of freezing rain in 31 h.

Given the catastrophic consequences associated with the 24–26 January 2017 ice storm over NB, this study aims to investigate the meteorological conditions that contributed to significant power outages during this event. Analyses of the storm were conducted using a high-resolution simulation (~1 km) with the Global Environmental Multiscale (GEM) model (McTaggart-Cowan et al. 2019) and available station observations. The analysis of the meteorological factors such as wind speed, precipitation amounts, and types and

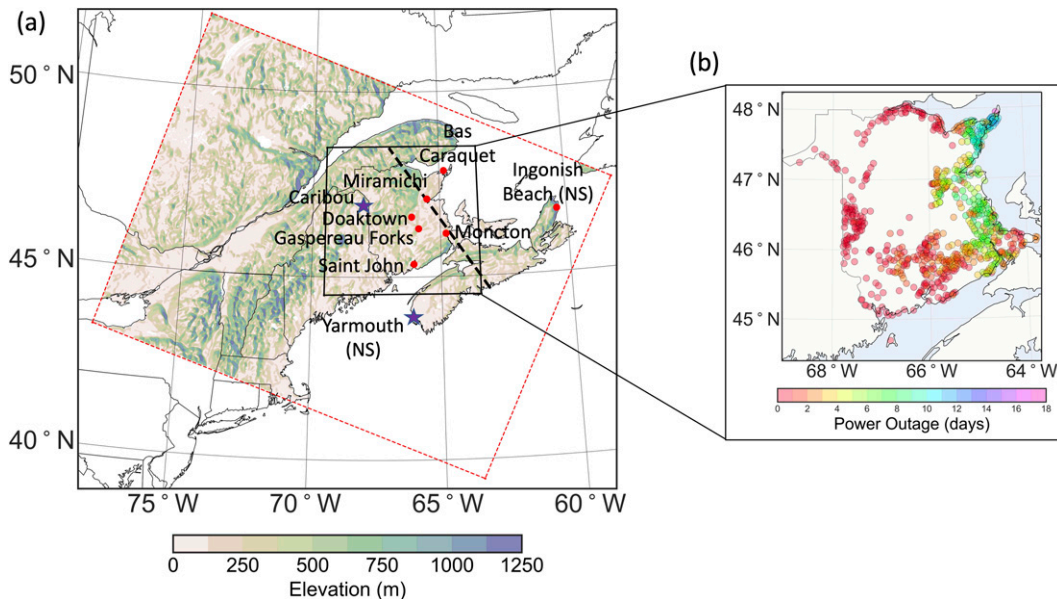


FIG. 2. (a) Map of eastern Canada, including southeastern Québec, New Brunswick (the black square), and the Maritime Provinces. Also shown are the simulation domains (red dotted line) with shaded orography (m) and the cross-sectional transect (black dashed line) across eastern NB. The red dots are the stations mentioned in the study. (b) Location and duration (days) of power outages resulting from the 24–26 Jan 2017 ice storm.

temperature are correlated with the amount of icing in regions of prolonged power outages.

The paper is organized as follows: [section 2](#) describes the simulation configuration and data analysis. [Section 3](#) provides a synoptic overview of the storm and compares the simulation outputs of the distributions, amounts, and types of precipitation with the observations. [Section 4](#) evaluates the relationships between the meteorological conditions, the electricity transmission network, and the duration of power outages. [Section 5](#) presents our conclusions.

2. Experimental design

a. Simulation configuration

The Canadian numerical weather prediction GEM model ([Girard et al. 2014](#); [Milbrandt et al. 2016](#); [McTaggart-Cowan et al. 2019](#)), version 4.8, was used to simulate the storm. The free simulation domain comprises 1296×1004 grid points at a grid spacing of 0.009° ([Fig. 2](#)). The simulation started at 0000 UTC 24 January 2017 and ended at 0000 UTC 27 January 2017, encompassing the duration of the storm over the Maritime Provinces. A time step of 30 s and an output frequency of 1 h were used. GEM uses hybrid log-hydrostatic pressure coordinates depending on the terrain and contains 62 staggered vertical levels that separate motion equations from thermodynamic equations in order to reduce noise ([Girard et al. 2014](#)). The simulation is driven each hour at the boundaries by the ERA5 Reanalysis ([Hersbach et al. 2020](#)), which uses a grid spacing of 0.25° and a temporal resolution of 1 h.

The Predicted Particle Properties (P3; [Morrison and Milbrandt 2015](#)) bulk microphysics scheme was used for clouds and precipitation processes. It predicts the mass and number mixing ratios of three hydrometeor categories: two liquid categories (viz., cloud droplets and rain) and one ice category. The distribution of the ice particles is a function of four prognostic variables that can evolve freely over several growth processes, from ice cloud initiation to complete riming through vapor deposition and partial riming. In addition to total ice mass and number mixing ratios, variables also include rimed ice mass and volume mixing ratios. The main microphysical processes that are parameterized for the ice category are ice nucleation, sublimation, and deposition at temperatures below 0°C , heterogeneous and homogeneous freezing, contact freezing, melting, collection with liquid particles (droplets and raindrops), and sedimentation.

In addition to the microphysical processes, other physical parameterizations included the correlated- k terrestrial and solar radiation scheme from [Li and Barker \(2005\)](#), a turbulent kinetic energy closure planetary boundary layer and vertical diffusion ([Benoit et al. 1989](#); [Delage and Girard 1992](#); [Delage 1997](#)), the Kuo-transient shallow convection parameterization ([Kuo 1965](#); [Bélair et al. 2005](#)), and the Interactions between Soil, Biosphere, and Atmosphere (ISBA) land surface scheme ([Bélair et al. 2003](#)).

The near-surface meteorological outputs used in the analysis were 2-m temperature and specific humidity, 10-m horizontal

wind speed and direction, sea level pressure, and the amount and type of precipitation. Total amounts of precipitation were divided into three categories: total, liquid, and solid. For precipitation types, freezing rain is diagnosed using the occurrence of rain at 2-m temperatures of less than 0°C . Ice pellets, in contrast, are diagnosed when solid accumulation occurs while there is a melting layer aloft and the 2-m temperature is less than 0°C . The diagnostic for identifying freezing rain and ice pellets is applied at an output frequency of 1 h. Atmospheric variables aloft include temperature, specific humidity, geopotential heights, horizontal and vertical winds, and the prognostic variables for ice, clouds, and rain from P3.

b. Datasets and data analysis

Data analyses were conducted in four steps, primarily using the high-resolution simulation outputs and surface station observations. We also used information provided by NB Power about 191 power outages that were recorded across NB ([Fig. 2](#)) during and after the storm.

First, model outputs were compared with observations from 241 stations within the model domain. These data were primarily compiled from locations (both manual and automated) managed by Environment and Climate Change Canada's Atlantic Regions division, supplemented by METAR reports gathered from the Wyoming Weather web (<http://weather.uwyo.edu/surface/>). Simulated vertical temperature and moisture profiles were evaluated against soundings from Caribou, Maine, prior to the storm (1200 UTC 24 January 2017), and approximately 1 h after precipitation started on the east coast of NB (1200 UTC 25 January 2017). These were used to identify the meteorological factors that contributed to the severity of the storm and to identify areas of interest for further research. In addition, the simulated soundings were also used to evaluate the model and to determine whether it could be used for fine-scale analysis of the storm.

Second, the vertical evolution of the hydrometeor distributions was analyzed at times when freezing rain and ice pellets were diagnosed along a vertical cross section perpendicular to the precipitation-type transition zone. The vertical cross section follows a transect, starting southeast of the Bas-Saint-Laurent region in Quebec, which traverses southeastward, toward coastal Nova Scotia. This transect also bisects the town of Miramichi, which experienced a substantial amount of freezing rain ([Fig. 2](#)).

Third, to investigate the horizontal distribution of icing on various structures, such as electrical transmission lines, ice accretion was computed offline using the technique provided by [Jones \(1998\)](#) because ice accretion is not an output from the simulation. [Jones \(1998\)](#) was chosen because it is widely used in the literature (e.g., [Rezaei et al. 2016](#); [Jeong et al. 2018](#)) and only requires information that is available from the simulation outputs, allowing computation of estimated icing amounts over the entire domain. The model [Eq. (5) in [Jones \(1998\)](#)] uses precipitation rate (mm h^{-1}) and 10-m wind speed (m s^{-1}) to estimate the uniform radial thickness of ice (in mm) around a cylindrical body (e.g., an electrical transmission line). The model assumes that the raindrop collection efficiency is 1,

ice is evenly distributed over the cable, and all of the liquid water that comes into contact with the cable freezes. Also, the model assumes an accreted ice density of 0.9 g cm^{-3} . Jones (1998) used the formula from Best (1949) to derive the liquid water content from the precipitation rate.

To highlight the key meteorological factors that affect the location and duration of power outages across NB, we investigated the correlations between ice accretion, freezing rain accumulation, 10-m wind speeds, proximity to the coast, the temperature regime, and the NB Power distribution and transmission network. The near-surface conditions that maintained freezing rain for up to 31 h were also studied. In particular, hourly near-surface thermal advection was computed using GEM simulation outputs at the grid point closest to each observation station. The 2-m temperature and 10-m horizontal wind speed and direction were analyzed. Temperature data were smoothed by averaging over 10-km^2 areas to avoid erroneous advection values near areas of complex orography (McCray et al. 2019). Equation (5) from Lackmann et al. (2002) was used to diagnose and analyze the latent heat release from the freezing of freezing rain at the surface. The estimated icing amount (icing_{mm}; mm) leading to a given change in temperature ΔT_{fzp} is

$$\text{icing}_{\text{mm}} \cong 0.05 F_A^{-1} \Delta T_{\text{fzp}} \Delta P_{\text{layer}_{\text{hPa}}}, \quad (1)$$

where $\Delta P_{\text{layer}_{\text{hPa}}}$ is the atmospheric layer through which the heat is distributed (100 hPa, estimated from the transect cross section) and F_A is the fraction of heat that warms the environmental air near the surface (0.75).

3. Overview of the storm

a. Synoptic-scale overview

The synoptic-scale pattern for 24–26 January 2017, shown in Fig. 3, depicts a typical winter storm associated with freezing rain across NB. There was a 200-hPa ridge over the Maritime Provinces at 1200 UTC 24 January 2017. A negatively tilted trough, oriented from northwest to southeast, moved across the northeastern coast of the United States. Relatively strong warm-air advection at 850 hPa ahead of the low pressure system contributed to the movement of the sea level low pressure system along the coast. Southerly winds at 850 hPa transported the moisture necessary for producing precipitation across the region.

The synoptic-scale pattern observed here corresponds to the “warm-front-occlusion sector of cyclones” pattern described by Rauber et al. (2001). Favorable conditions for freezing rain/ice pellets (Fig. 3) occurred when warm-air advection created a melting layer aloft ($T > 0^\circ\text{C}$), and a cold layer ($T < 0^\circ\text{C}$) was formed through low-level cold-air advection near the surface. The low pressure system weakened as it moved slowly northeastward along the east coast of the United States and Nova Scotia until it reached southwest Nova Scotia (Fig. 4). The low pressure system then deepened once it started to move northward, which coincided with the end of precipitation over NB.

The measured vertical atmospheric conditions during the storm are shown in Fig. 5. Upper-air observations from Caribou exhibit a profile of increasing temperature with height up to ~ 750 hPa at 1200 UTC 24 January 2017. Warm-air advection produced a melting layer aloft, that is then measured at 1200 UTC 25 January 2017. Depending on the surface temperature (Stewart et al. 2015), a combination of ice pellets and liquid precipitation (rain or freezing rain) could have been produced at these times. The sounding at 1200 UTC 25 January 2017 is well reproduced overall, particularly between 1000 and 800 hPa and above 700 hPa, but it missed the warm layer aloft. The model data interpolation on standard pressure levels (i.e., the lack of data between 850 and 700 hPa) or lower warm-air advection aloft could explain why the shallow warm layer aloft was not well simulated. Note that the two dry layers at 900 and 600 hPa were not captured by the model but were measured at both Caribou and Yarmouth, Nova Scotia (not shown), during the storm. At both times, the simulated temperatures at lower levels (pressures > 850 hPa) are similar to the measurements. The near-surface temperatures are 2.2°C colder on 1200 UTC 24 January 2017 and 0.3°C warmer on 1200 UTC 25 January 2017.

The time evolution of simulated 2-m temperatures and 10-m winds during precipitation on the east coast is shown in Fig. 6. Prior to the storm, at 1200 UTC 24 January 2017, the 2-m temperatures were mainly less than 0°C across NB (not shown). As the low pressure system moved northeastward, warm air ($>0^\circ\text{C}$) started to reach Nova Scotia and southern NB at 0000 UTC 25 January 2017. Subsequently, southern NB was associated with 2-m temperatures above 0°C throughout the storm whereas northern NB was associated with colder 2-m temperatures ($< -2^\circ\text{C}$). Central NB, near the eastern coast, the 2-m temperatures were near 0°C [between -2° and 2°C as in Mekis et al. (2020)] for the duration of precipitation. The simulation had a 2-m temperature mean bias of -0.16°C for the 48-h period for the 20 stations in NB. The bias varied from -1.34° to $+0.74^\circ\text{C}$, with the 2-m temperature bias generally at around -1°C during freezing rain.

b. Precipitation fields

At 1200 UTC 24 January 2017, the warm-air layer aloft started to reach southern NB. The wind direction had a weak northerly component at lower levels and a southerly component at 850 hPa (Figs. 3 and 5), consistent with the evolution of the $>0^\circ\text{C}$ layer. Precipitation started to reach the surface as freezing rain and ice pellets at 1800 UTC 24 January 2017 in southern NB (not shown). The main pulse of precipitation started at 1600 UTC 24 January 2017 over southwestern NB and Nova Scotia and lasted until around 2000 UTC 25 January 2017 over northeastern NB. Isolated postfrontal convective activity produced scattered showers across NB until 0800 UTC 26 January 2017 (not shown). During the 31 h of sustained precipitation, more than 100 mm of precipitation was reported over the Maritime Provinces (Fig. 7). The largest value recorded for total precipitation was 127 mm at Ingonish Beach, Nova Scotia, which was well reproduced by

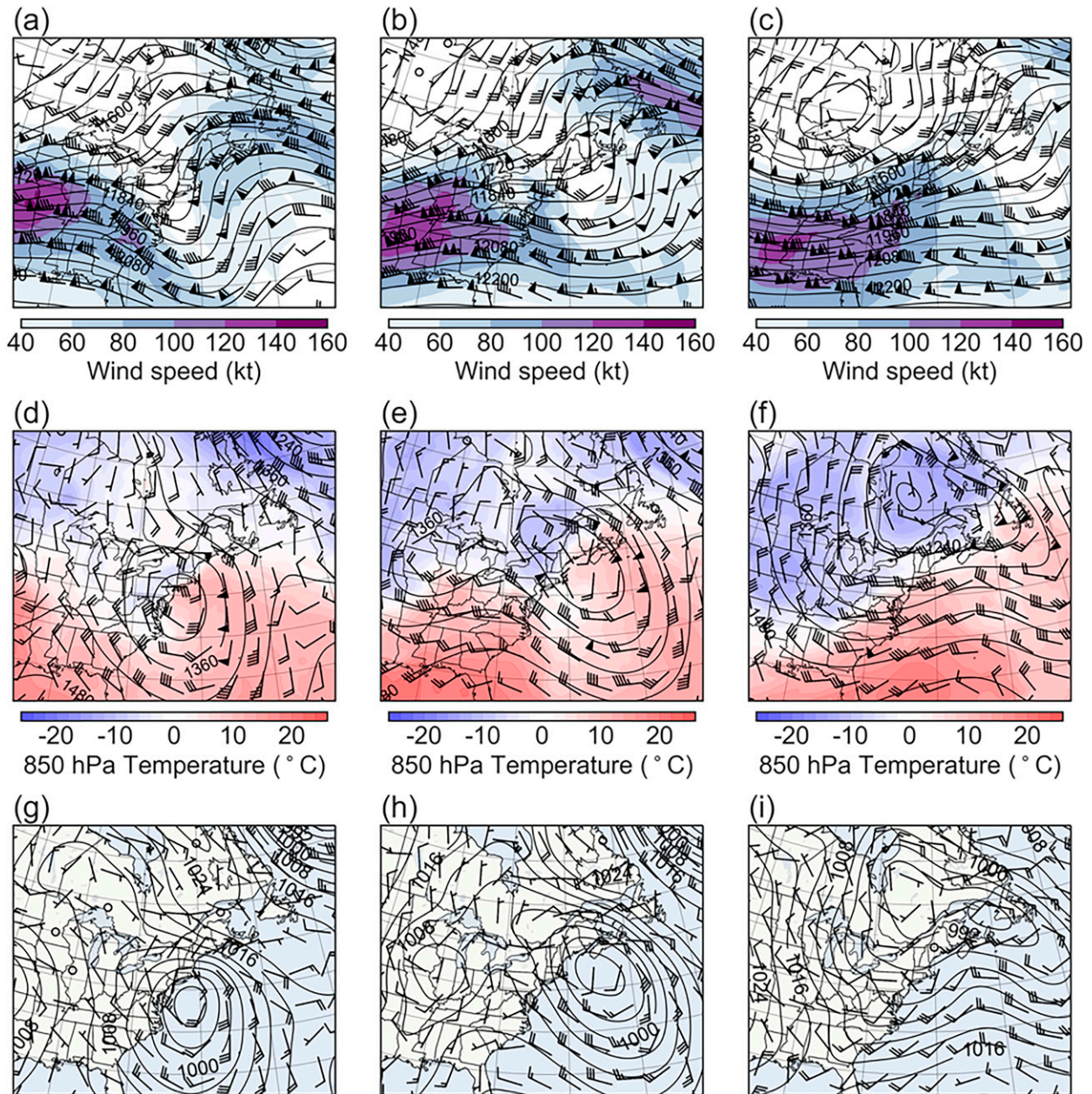


FIG. 3. Time evolution of the synoptic-scale conditions at (left) 1200 UTC 24, (center) 1200 UTC 25, and (right) 1200 UTC 26 Jan 2017, showing ERA5 reanalysis of (a)–(c) upper-level geopotential heights at 200 hPa (black lines, every 60 m), 200 hPa wind barsbs and wind speeds (colors; kt, 1 kt $\approx 0.51 \text{ m s}^{-1}$), (d)–(f) 850-hPa geopotential heights and isotherms, and (g)–(i) the corresponding mean sea level pressure (black solid lines, every 4 hPa), the 1000–500 hPa thickness (dashed blue and red lines, every 60 m), and the 10-m wind barsbs [using the standard increments of 50 (flag), 10 (full barb), 5 (half barb) kt and open circles for calm conditions].

the simulation. In NB, 85 mm of liquid water equivalent was recorded on the southern part of the coast (near Saint John, NB), with a maximum observation of 101 mm at Gaspereau Forks (central-southern NB).

The largest amounts of freezing rain were observed in northeastern NB. The distribution of freezing rain along the coast was well reproduced by the model, in particular at Miramichi. More freezing rain, however, was observed at Bas

Caraquet relative to the simulations. Across the 240 stations, the simulation generally underestimated total precipitation values with a mean bias of -2.53 mm (Fig. 7). Conversely, freezing rain was overpredicted, with a bias of 12.17 mm (Fig. 7). This bias could be due to a lack of observations, with only eight stations that measured freezing rain. Simulated freezing rain was used in the remainder of the study, given the low number of stations.

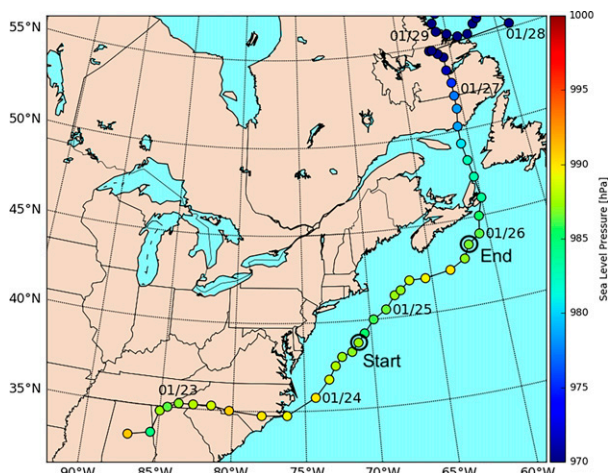


FIG. 4. Three-hourly time evolution from 1200 UTC 22 Jan to 0300 UTC 29 Jan 2017 of the observed near-surface pressure (colors; hPa). The two black circles indicate when the main pulse of precipitation started and ended over New Brunswick. The storm track was computed using ERA5 and the algorithm for midlatitude low-pressure systems by Chartrand and Pausata (2020).

c. Precipitation-type transitions

The precipitation types that reach the surface depend on the characteristics of the melting layer aloft and a refreezing layer below it. The temperature fields aloft are shown in Figs. 8 and 9 along the cross section shown in Fig. 2. At 2100 UTC 24 January 2017, the melting layer aloft and a refreezing layer below extended throughout the entire cross section, with precipitation only occurring south of Miramichi. At 0000 UTC 25 January 2017, southerly winds aloft advected warm air and the height of the upper boundary of the melting layer increased to 3 km. At the same time, northeasterly winds transported relatively cold air near the surface and a peak in freezing rain was observed southeast of Miramichi, at

approximately -175 km. At 0300 UTC 25 January, the southern edge of the refreezing layer moved northward to -200 km. Also, the depth of the melting layer aloft increased to ~ 1.5 km at Miramichi until 0900 UTC 25 January 2017. At 0900 UTC 25 January 2017 north of Miramichi, the depth of the melting layer started to decrease to ~ 1 km until 1800 UTC 25 January 2017. This location corresponds with the location of a strong horizontal temperature gradient at 850 hPa (Fig. 3). At that time, while the location of the melting layer aloft remained relatively constant, the southern edge of the refreezing layer moved northward until 1500 UTC 25 January 2017. At 0600 UTC 25 January 2017, the maximum temperature of the melting layer aloft was 8.7°C , which is greater than the melting-layer maximum temperature recorded during the 1998 ice storm over southern Quebec (Cholette et al. 2020). The melting layer aloft produced by the simulation was 1.5 km deep, comparable to depths that were simulated and observed in 1998 (Cholette et al. 2020). Although the depth of the melting layer aloft during the 1998 ice storm reached 2.5 km over southern Quebec, in general, melting-layer depths greater than 1.5 km are not commonly observed (Zerr 1997).

The precipitation-type transition region, which is bounded by regions of only rain and only snow, migrated from south to north with the movement of the melting layer aloft (Figs. 8 and 9). Heavy precipitation occurred over NB between 0000 and 1200 UTC 25 January 2017. The width of the transition region decreased from 250 to 100 km from 0000 to 0600 UTC 25 January 2017 and remained ~ 100 km wide until 1200 UTC 25 January 2017. This area of precipitation is slightly narrower than that throughout the 1998 ice storm, which was nearly 161 km wide over southern Quebec (Cholette and Thériault 2021). Freezing rain occurred within this transition region as rain changed to freezing rain when the 2-m temperatures decreased to less than 0°C . The rain-to-freezing rain transition moved northward at ~ 25 km h^{-1} from 0000 to 0600 UTC 25 January 2017, slowing to 8 km h^{-1} from 0600 to 1200 UTC 25 January 2017.

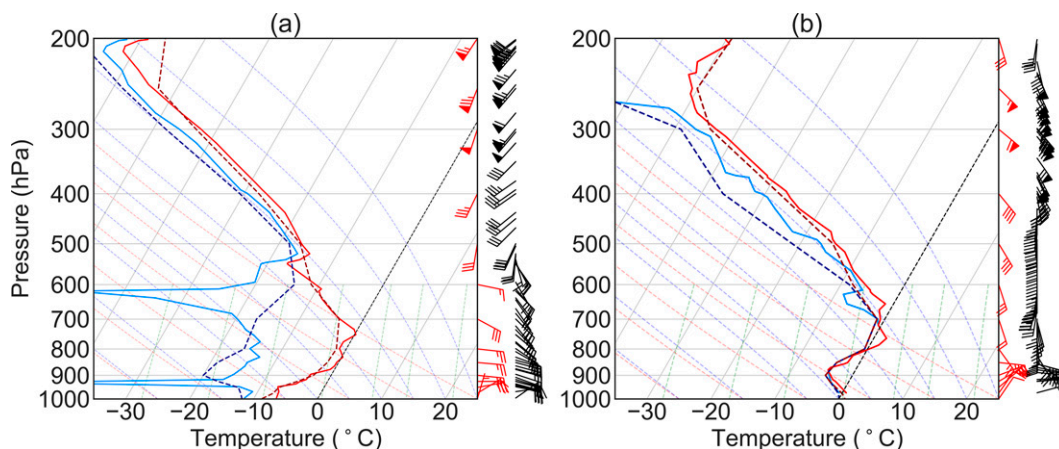


FIG. 5. Observed (solid) and simulated (dashed) vertical profiles of temperature (red; $^{\circ}\text{C}$) and dewpoint temperature (blue; $^{\circ}\text{C}$) at (a) 1200 UTC 24 and (b) 1200 UTC 25 Jan 2017 in Caribou. The red wind barbs are simulations, and the black wind barbs are measurements. Observed profiles are from the University of Wyoming website (<http://weather.uwyo.edu/>).

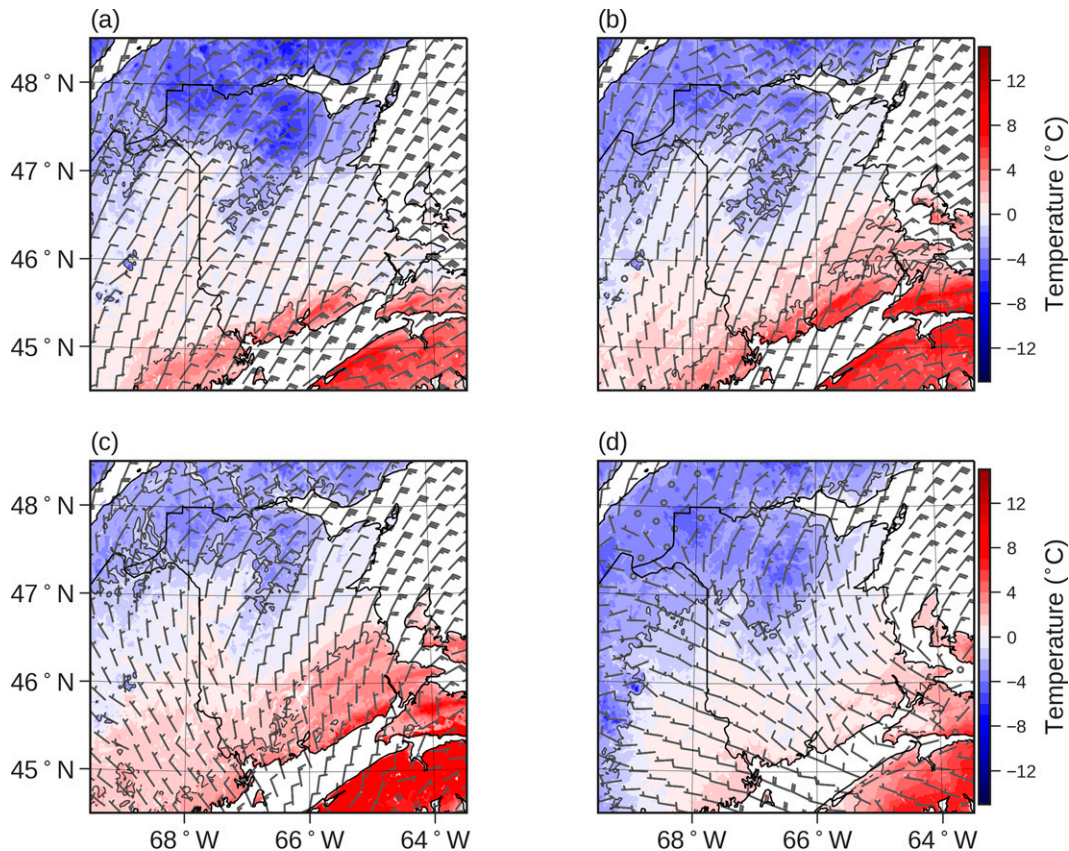


FIG. 6. The simulated time evolution of the 2-m temperature (colors; °C) and 10-m horizontal wind barsbs (same legend as in Fig. 3) over New Brunswick during the hours of highest freezing precipitation rates at (a) 0600 UTC 25, (b) 1200 UTC 25, (c) 1800 UTC 25, and (d) 0000 UTC 26 Jan 2017.

d. Clouds and precipitation aloft

The different hydrometeors formed aloft influences the surface precipitation types and properties (Figs. 8 and 9). Freezing rain was mainly produced by the complete melting of ice aloft (Stewart et al. 2015). Ice particles were present aloft throughout the storm along the entire cross section, except at 1800 UTC 25 January 2021. The amount of ice mass aloft depends on the deposition growth rate and the interaction of ice particles with cloud droplets. The amount of cloud droplets increases when supersaturation is reached, due to diabatic cooling from phase changes and by adiabatic cooling associated with ascending air. The ice mixing ratio, cloud droplets, and vertical air motion are shown in Figs. 8 and 9.

The intensity of freezing rain produced by melting ice particles varied along the cross section (Figs. 8 and 9). At 0000 UTC 25 January 2017 at approximately -160 km, the freezing rain rate was between 4 and 8 mm h⁻¹ and the amount of ice aloft was relatively high (>1 g m⁻³). This was the case until 0900 UTC 25 January 2017, when the ice mixing ratio aloft decreased (<0.5 g m⁻³), reducing the precipitation rate to 2 – 4 mm h⁻¹, illustrating that freezing rain rates at the surface are often contingent on ice amounts aloft.

In addition to the amount of ice, the degree of riming also influences precipitation at the surface. First, ice pellets, which are rimed ice particles produced in the refreezing layer from partially melted ice aloft, were diagnosed at the surface from 2100 UTC 24 January 2017 until 1200 UTC 25 January 2017. Unlike freezing rain, ice pellets were consistently present through a narrow region at the surface below the northern edge of the melting layer, as previously shown by Thériault et al. (2006). Second, large amounts of riming in the melting layer can produce high rates of freezing rain at the surface. Both scenarios were present near Miramichi at 0300 UTC 25 January 2017. The maximum rime mass fraction (0.8 – 1) was produced south of Miramichi within the melting layer aloft and is associated with the highest rate of freezing rain at the surface (8 mm h⁻¹). High rime mass fraction values were also present at lower elevations (<2 km) north of Miramichi, characterizing ice pellets in the refreezing layer and at the surface. The horizontal transport of hydrometeors also influenced the distribution of precipitation types, especially between 0600 and 0900 UTC 25 January 2017. The ice mass content aloft increased and reached the surface between 50 and 100 km north of Miramichi. Some of this ice aloft was transported northward by southerly winds, and at lower elevations, the ice was advected southward by northerly winds.

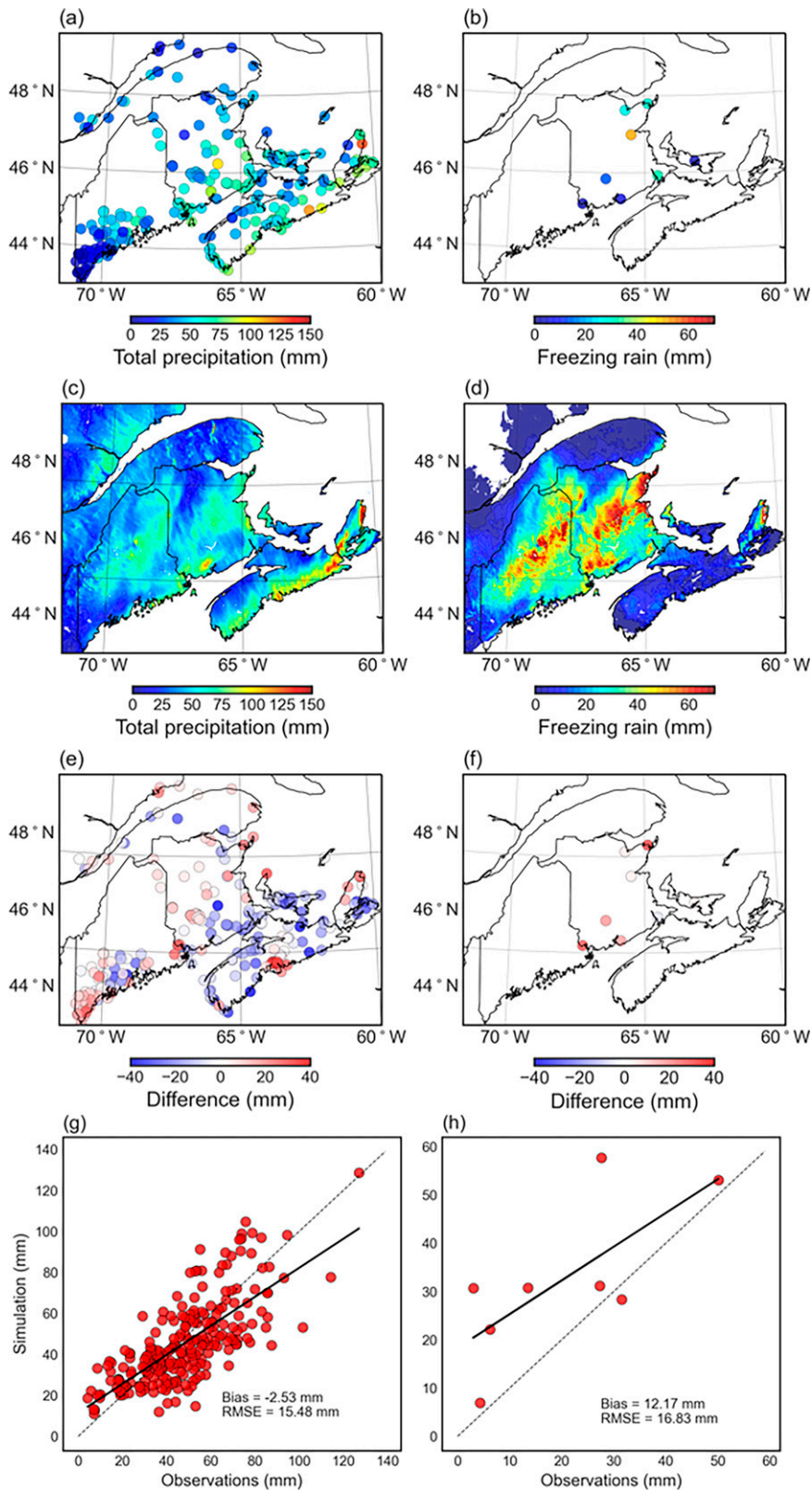


FIG. 7. Total amount of (left) precipitation and (right) freezing rain simulated and measured from 0000 UTC 24 to 0000 UTC 27 Jan 2017, showing (a),(b) observed and (c),(d) simulated; (e),(f) simulated minus observed; and (g),(h) a comparison between simulated (at the nearest grid point to the observation) and observed. Only eight stations recorded freezing rain in New Brunswick.

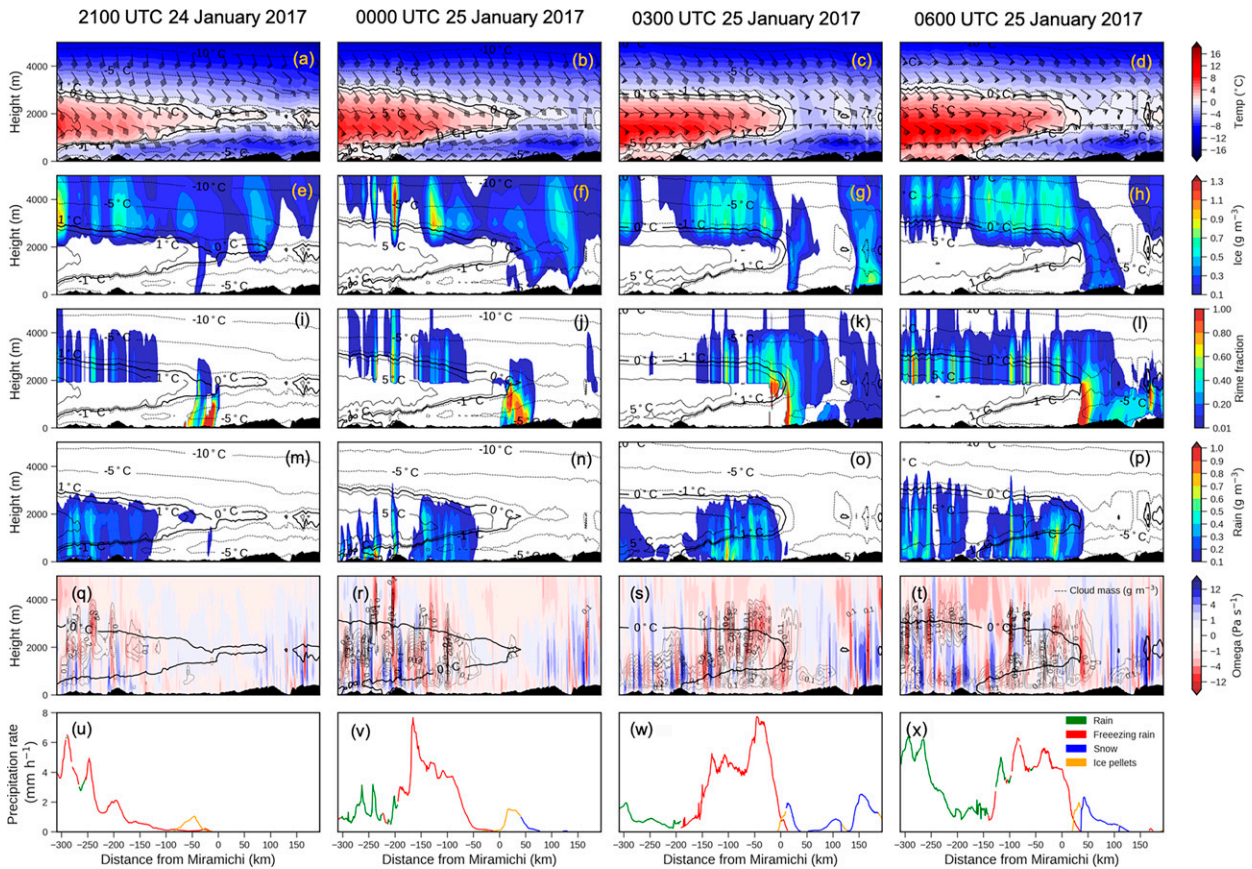


FIG. 8. (a)–(d) The temperature ($^{\circ}\text{C}$) and horizontal wind bars (using the same legend as in Fig. 3), (e)–(g) ice mass content (g m^{-3}), (i)–(l) rime mass fraction, (m)–(p) rain mass content (g m^{-3}), (q)–(t) cloud mass content (solid lines; g m^{-3}) and vertical air motion (colors; Pa s^{-1}), and (u)–(x) surface precipitation rate (mm h^{-1}) of rain (green), freezing rain (red), snow (blue) and ice pellets (orange) along the cross section shown in Fig. 2a. Temperature contours (black lines, every 5°C) are shown in (a)–(p), and a 0°C isotherm (thick black line) is shown in (q)–(t). Times shown are (left) 2100 UTC 24 Jan and (left center) 0000 UTC, (right center) 0300 UTC, and (right) 0600 UTC 25 Jan 2017.

At 0900 25 January 2017, the relatively colder melting layer aloft led to a combination of freezing rain and ice pellets at the surface. A portion of these ice pellets were advected southward below the melting layer, as indicated by the presence of more ice 80 km north of Miramichi. The rime mass fraction was > 0.8 between 50 and 125 km.

Warm rain processes also produced freezing precipitation at the surface. At 1200 UTC 25 January 2017, the northern edge of the melting layer aloft extended to 50 km north of Miramichi. At that time, freezing rain extended farther north (up to 100 km), which is explained by the presence of warm rain processes aloft (Rauber et al. 2000; Kochtubajda et al. 2017; Lu et al. 2022). Supercooled rain was also formed aloft at 1500 UTC 25 January 2017. The interaction between the ice crystals and supercooled rain produced rime ice particles. These processes occurred at the end of the precipitation period as rates decreased to less than 2 mm h^{-1} from 1800 UTC 25 January 2017 onward.

In summary, a deep and warm melting layer aloft extended northward throughout the storm. Combined with the presence of a persistent refreezing layer due to northerly

surface winds, freezing rain, ice pellets, and a mixture of both were produced along the cross section and throughout eastern NB. Precipitation lasted more than 15 h over Miramichi, starting with ice pellets for a duration of 3 h from 0000 UTC 25 January 2017, followed by a combination of freezing rain and ice pellets for another 3 h, and by freezing rain from 0600 to 1500 UTC 25 January 2017. Large amounts of ice particles were rimed aloft and in the refreezing layer near the surface, because of the presence of cloud droplets that increased the rime mass fraction of ice (Figs. 8 and 9). The increase in ice mass fraction leading to ice pellets, for example, were simulated by two processes. First, wet growth of ice particles occurs from the collected cloud droplets, and second, from heterogenous freezing of cloud droplets at temperatures less than -5°C . In Cholette et al. (2020), the rime mass fraction of ice pellets that were formed in the refreezing layer is high due to the refreezing process of partially melted ice particles. This process was not simulated in our study and the increase in the rime mass fraction during the storm is only due to the freezing of cloud droplets that are collected by the unmelted ice particles.

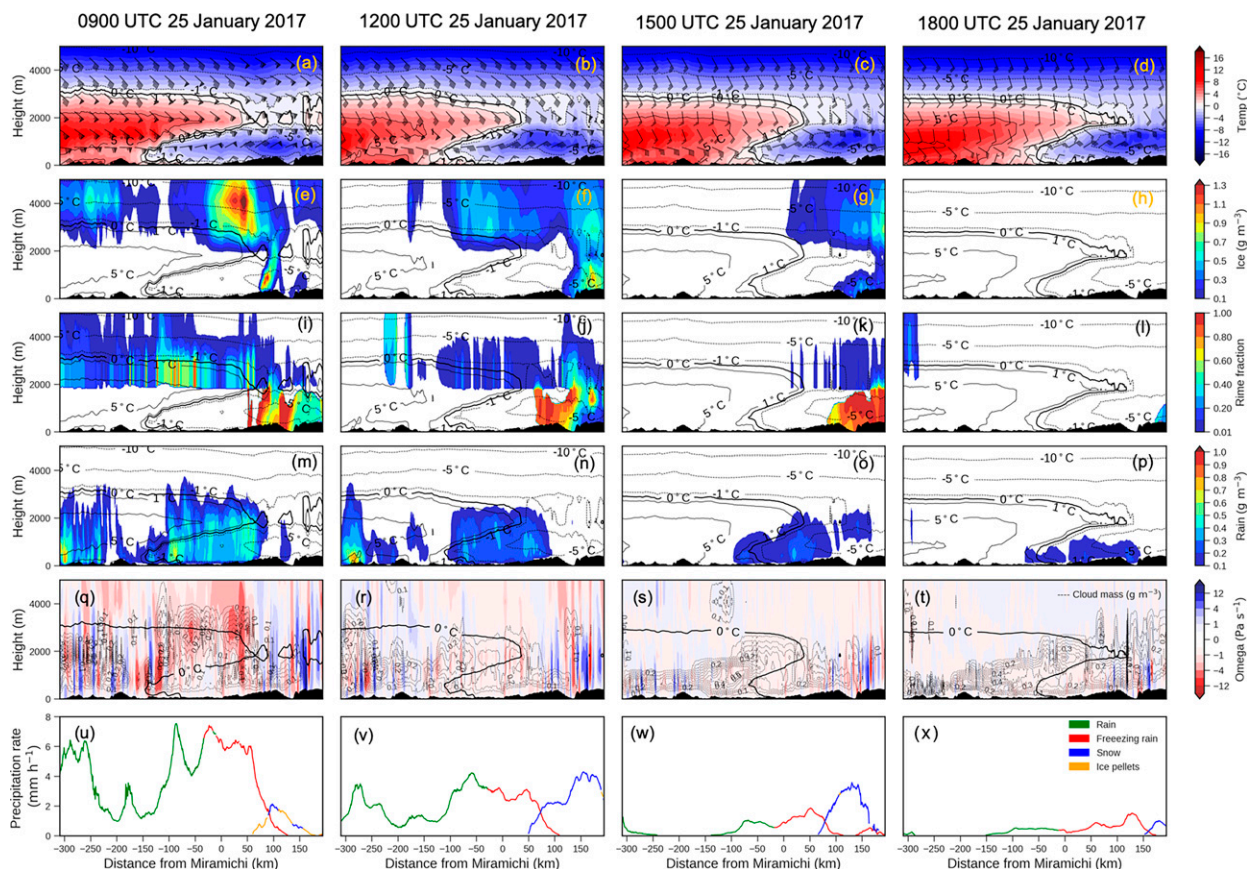


FIG. 9. As in Fig. 8, but at (a),(e),(i),(m),(q),(u) 0900 UTC; (b),(f),(j),(n),(r),(v) 1200 UTC; (c),(g),(k),(o),(s),(w) 1500 UTC; and (d),(h),(l),(p),(t),(x) 1800 UTC 25 Jan 2017.

4. Factors that impacted the duration of power outages

a. Icing and duration of power outages

Ice accumulation on structures, especially electrical transmission and distribution infrastructure, is associated with a combination of freezing rain and moderate to strong winds at the surface. Power outages can occur when large amounts of ice accumulate on these networks. The duration of the power outages caused by the January 2017 storm was proportional to the amount of freezing rain accumulation in each region, which increased northeastward (Figs. 2 and 7d). The maximum relative accumulation of freezing rain (Figs. 7b,d) and power network disruption (Fig. 2) occurred in northeastern NB.

The fraction of the total precipitation across the province of NB that is attributed to freezing rain is shown in Fig. 10a, along with the power distribution network. Freezing rain made up a large portion of the total precipitation throughout the storm when 2-m temperatures were near 0°C (Fig. 10b). Freezing rain that reached northeastern NB, however, was mainly associated with 2-m temperatures of <0°C. Southern NB, located in the warm sector of the low pressure system, received less freezing rain relative to the total amount of precipitation. This is mainly because the 2-m temperatures increased rapidly above 0°C and precipitation

changed to rain during daytime, even in locations with long periods of precipitation. This region experienced shorter-duration power outages despite the dense distribution network. In contrast, northeastern NB received more precipitation, mainly in the form of freezing rain, and experienced longer power outages as a result.

The duration of power outages was analyzed with respect to proximity to the coast, the average near-surface wind speed during the storm, and the fraction of freezing rain of the total precipitation (Fig. 11a). A Spearman rank-order correlation r_s was used to identify statistically significant relationships. Most long-duration power outages (>5 days) were located within 20 km of the NB coast, and the power outage durations decreased farther away from the coast ($r_s = -0.365$; $p < 0.01$) (Fig. 11a). This is consistent with results from Stuart and Isaac (1999) and Cortinas et al. (2004), who found that the number of annual freezing rain hours were higher near the coast than inland. However, Chartrand (2020) found that the maximum amount of accumulated freezing rain occurred southeast of NB and not in northeastern NB, as observed during the storm in our study. For 24–26 January 2017, despite a greater fraction of the total precipitation in the interior of the province being freezing rain, amounts were lower than along the coast (Fig. 7).

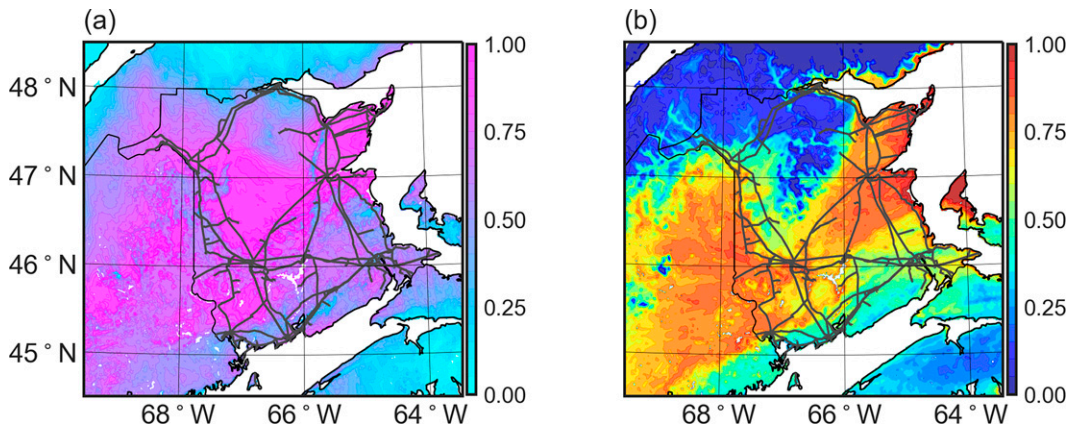


FIG. 10. Simulated fraction (from 0 to 1) of (a) freezing rain from the total precipitation across New Brunswick and surrounding areas from 0000 UTC 24 Jan to 0000 UTC 27 Jan 2017 and (b) hours with 2-m temperatures between -2° and 2°C from all hours with precipitation for the same period as (a). Dark-gray lines represent the NB Power transmission network.

Winds became weaker farther away from the coast. Most locations associated with strong winds ($>25\text{ km h}^{-1}$) were situated within 2 km of the coast, except in a few sheltered coastal areas. For locations near the coast ($<2\text{ km}$), the duration of power outages also increased with the fraction of freezing rain of the total precipitation ($r_s = 0.486$; $p < 0.01$). All areas that experienced power outages of nine days or more were associated with fractions of freezing rain that were above 0.8 ($>80\%$) and winds of $>25\text{ km h}^{-1}$. A comparison of average measured wind speeds during seven other storms that caused power outages (Chartrand 2020) in the region with those from this storm showed that wind speeds $>25\text{ km h}^{-1}$ are common during freezing rain along the coast (not shown).

There is a strong correlation between the mean 2-m temperature and the range in 2-m temperature with accumulated freezing rain ($r_s = -0.639$; $p < 0.01$) (Fig. 11b). The range in the 2-m temperature is the maximum minus the minimum

temperature, simulated during freezing precipitation, therefore the duration is location dependent. In general, the longer the precipitation persisted, the wider the range of 2-m temperatures was ($r_s = 0.438$; $p \leq 0.01$), and the more likely it was to transition into other precipitation types. Thus, this produced less freezing rain and more rain. Conversely, a warmer mean ($>-1.5^{\circ}\text{C}$) ($r_s = 0.650$; $p \leq 0.01$) with a narrower range of 2-m temperatures ($r_s = 0.715$; $p \leq 0.01$) was associated with shorter durations and more freezing rain.

b. Time series of weather conditions and ice accumulation

Near- 0°C conditions commonly occurred during the storm (Figs. 6 and 11b). As mentioned in section 3, the east coast of NB was associated with three distinct temperature and precipitation regimes. The time series of precipitation types, 2-m temperatures, icing, 10-m horizontal wind speed and direction, the

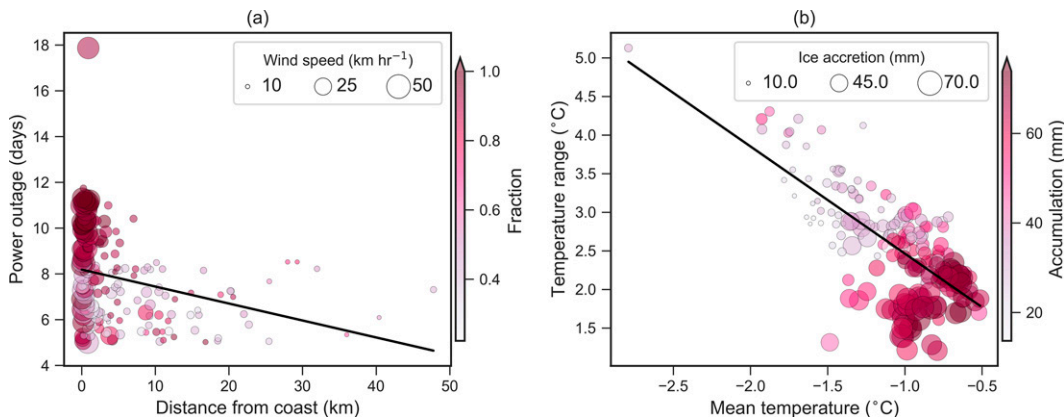


FIG. 11. Correlation of physical parameters. (a) Power outage duration (days) compared with proximity to the coast (km), with the fraction of freezing rain from total accumulation (shades of pink) and mean surface wind speeds (km h^{-1} ; size of circles) during freezing rain only, and (b) 2-m temperature range ($^{\circ}\text{C}$) compared with 2-m mean temperature ($^{\circ}\text{C}$) during freezing rain only, with freezing rain accumulation (mm; shades of pink) and modeled ice accretion (mm; size of circles) on circular conductors [using Eq. (5) of Jones (1998)].

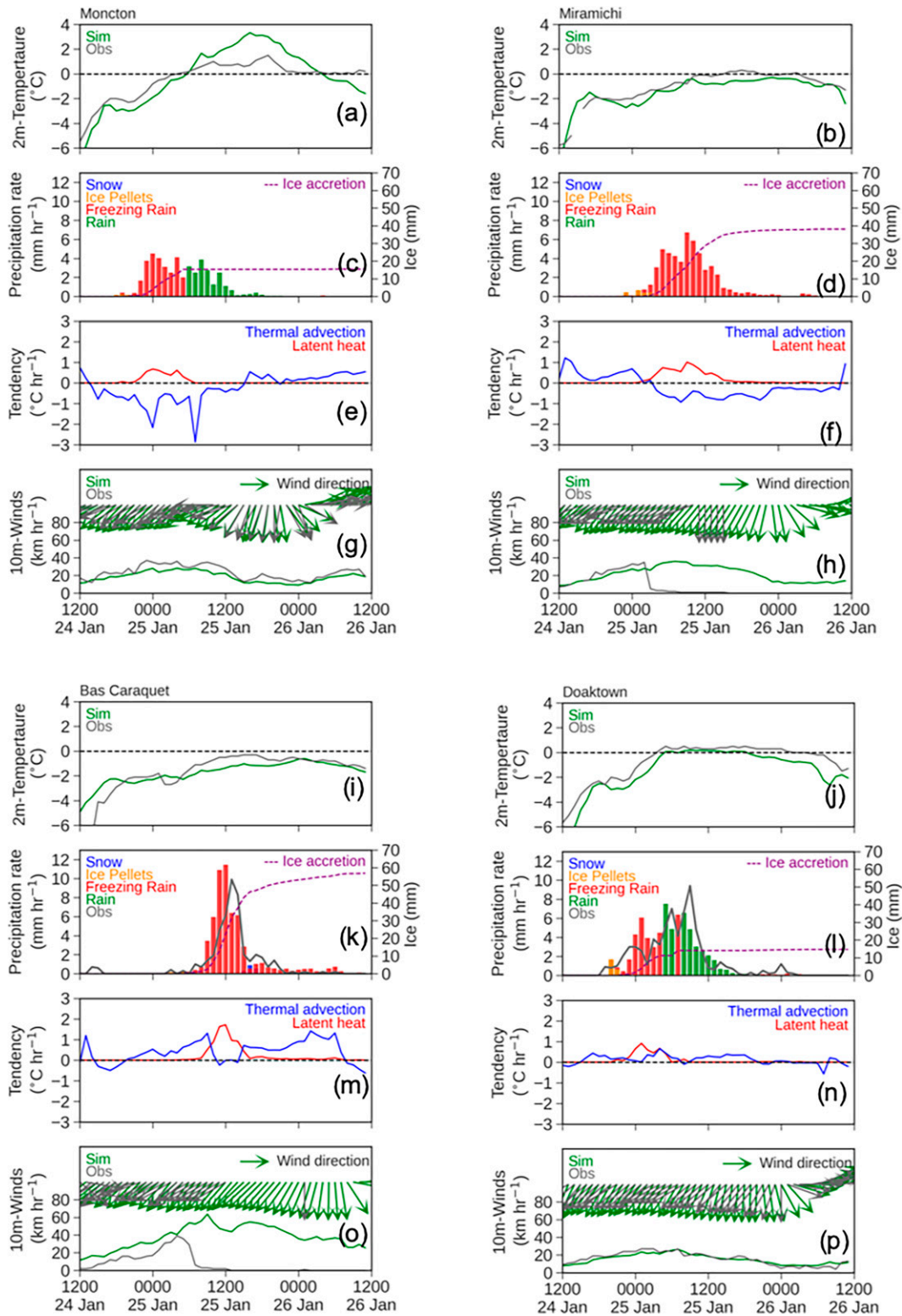


FIG. 12. Time series of (a),(b),(i),(j) simulated (green) and observed (black) 2-m temperature; (c),(d),(k),(l) observed surface precipitation rate (in black when available; mm h⁻¹), simulated surface precipitation rate (mm h⁻¹) of snow (blue), ice pellets (orange), freezing rain (red), rain (green), and the calculated ice accretion (dashed purple line; right y axis; mm); (e),(f),(m),(n) calculated thermal advection (blue) and latent heat of freezing (red) (°C h⁻¹) using the simulation; and (g),(h),(o),(p) simulated (green) and observed (black) 10-m horizontal wind directions (arrows)

thermal advection rate, and the heating rate from freezing of supercooled drops at the surface at four different locations (shown in Fig. 2) are shown in Fig. 12.

In southeastern NB, 2-m temperatures were generally higher south of Miramichi (Fig. 12), and precipitation types changed rapidly from freezing rain to rain (~4 h). At Moncton, the total accumulated freezing rain over 13 h was 21 mm (until 0500 UTC 25 January 2017), after which the 2-m temperature increased to >0°C for the following 24 h. During freezing rain, wind speeds were ~30 km h⁻¹ in both the simulation and the observations. Smaller amounts of ice accumulation were simulated in this region and power outages generally lasted around 5–8 days.

In eastern central NB, at Miramichi (Fig. 12), freezing rain started ~4 h later than at Moncton as the transition region migrated northward (Figs. 8 and 9). The 2-m temperature was slightly below 0°C during periods of precipitation. Approximately 38 mm of ice accumulated on structures during the freezing rain event that lasted between 27 and 30 h in the areas surrounding Miramichi, with simulated precipitation rates up to 7 mm h⁻¹ and observed easterly winds up to 40 km h⁻¹. These easterly winds would have been parallel to the Miramichi River as it entered Miramichi Bay.

In northeastern NB, freezing rain started at around 0500 UTC 25 January 2017, at Bas Caraquet (Fig. 12), ~5 h after Miramichi and with slightly lower temperatures. The duration of freezing rain at Bas Caraquet was similar to that at Miramichi, but the maximum rate was higher, at up to 11.5 mm h⁻¹. This led to a faster buildup of ice, assisted by stronger winds (up to 60 km h⁻¹), and led to major power outages (up to 11 days) as compared with the shorter-duration power outages around Miramichi (~9 days).

Although ice accretion using Jones (1998) was computed when simulated 2-m temperatures were less than 0°C, the locations presented in Fig. 12 are all associated with temperatures that approach or surpass 0°C during the storm. Two primary mechanisms may lead to an overestimation of icing using this method: (i) When simulated and observed temperatures diverge ice accretion continues in the model where it may have ceased in real-world conditions, as observed at Miramichi; and (ii), as pointed out by Makkonen (1998) and Yip (1995), near 0°C the efficiency of icing is <1, therefore, the modeled ice amount is probably overestimated when simulated temperatures are near, but below, 0°C. Other factors also not considered by Jones (1998) include spongy ice, the formation of icicles, and the uniformity of ice thickness.

c. Processes associated with near-0°C conditions

Along the east coast of NB, more frequent near-0°C conditions occurred with high fractions of freezing rain (Fig. 10). Warming associated with the release of latent heat from the freezing of supercooled drops (freezing rain) at the surface

increased the 2-m temperature to 0°C (Lackmann et al. 2002). This process is compared with the near-surface thermal advection, assuming that vertical air motion was near 0 m s⁻¹ near the surface (Fig. 12). The order of magnitude of the thermal advection is similar to the temperature tendency associated with the latent heat released by freezing at all stations, except at Moncton, where it is smaller.

The effect of latent heat released from freezing rain varied across NB (Fig. 12). First, in southern NB, only <1°C h⁻¹ of heating occurred over ~9 h, and it was combined with cold-air advection, which then changed to warm-air advection. Freezing rain changed to rain early in the morning and McCray et al. (2020) suggested that this is common during long-duration freezing rain storms. Other processes, such as cloud radiative transfer, vertical transport of warm air aloft through shear-induced mixing, and sensible heat transport from the falling rain, could also have contributed to the increase in temperatures above 0°C. Second, at Miramichi, the rate of warming released from freezing rain was ~1°C h⁻¹ over ~12 h. Even with more warming from the freezing process relative to Moncton, freezing rain did not change into rain. The relatively weak cold-air advection near the surface was strong enough to maintain the 2-m temperature at slightly below 0°C and sustain freezing rain. Chartrand (2020) showed that the cold air near the surface during freezing rain was associated with cold-air damming in the area due to the presence of the Appalachians to the west. This process is, however, weak during this storm in comparison with the events studied in Chartrand (2020). Third, 2-m temperatures reached -0.5°C for only a short period (2 h) of time at Bas Caraquet, despite the large amount of freezing rain that reached the surface. At Bas Caraquet, significant amounts of precipitation started at around 0800 UTC 25 January 2017 (morning), with precipitation rates quickly reaching >10 mm h⁻¹. The warming associated with particle refreezing at the surface was greater than 1°C for ~6 h. Then the temperature decreased by only 1°C during the night even with weak warm-air advection. At that time, relative humidity increases when combined with cooling could suggest sublimation of the ice coat. The nighttime radiational cooling could also contribute to the decrease in temperature. The pattern was different at Doaktown, located in the middle of NB. This station was colder than other locations along the coast before the onset of precipitation and only experienced warm-air advection. Consequently, freezing rain changed to rain at 0400 UTC 25 January 2017.

The contribution of the latent heat release during freezing rain events in the 24–26 January 2017 storm was compared with calculations from Henson et al. (2011) for the 1998 ice storm. As during the 1998 ice storm, the prolonged duration of freezing rain at Miramichi was likely maintained by cold-air advection near the surface. If cold-air advection is not considered, surface temperatures would have increased to 0°C

←
and speeds (lines) at Moncton, Miramichi and Bas Caraquet and also at Doaktown. Wind speeds at Miramichi from 0200 UTC 24 Jan 2017 [in (h)] and Bas Caraquet from 0600 TC 24 Jan 2017 [in (o)] are not measured because of suspected frozen anemometers (e.g., Ryerson and Ramsay 2007). Station locations are shown in Fig. 2.

within 5 h of the onset of freezing rain. This would have limited the freezing rain accumulation to only 4.8 mm instead of the 38 mm over 27 h that was observed. The processes were different inland at Doaktown (Fig. 12), where weak ($<1^{\circ}\text{C h}^{-1}$) warm-air advection that occurred near the surface contributed to maintaining temperatures at greater than 0°C for 5 h longer than if the warm-air advection had been zero. Without the warm-air advection near the surface, a second icing period at around 0000 UTC 26 January 2017 would have started 3–4 h earlier and contributed to an additional 10 mm of freezing rain accumulation.

A cold bias in the 2-m temperature of up to -1°C was produced during freezing rain at the four stations shown in Fig. 12. The warming from latent heat released from the freezing of supercooled drops at the surface played an important role during the storm, as noted in McTaggart-Cowan et al. (2019), particularly when a similar order of magnitude is estimated between the amount of thermal advection and latent heat release from freezing. This is the case at Miramichi, where the 2-m temperature is near 0°C throughout the period of the freezing rain. This feedback process, of supercooled drops freezing at the surface and the increasing of near-surface temperatures from the latent heat release, is not included in our simulation. Sensitivity studies should be conducted in future work to better understand these mechanisms.

Overall, precipitation types and storm severity can be impacted by small changes in temperature when the conditions are near 0°C . For example, at Miramichi, the observed 2-m temperature was just above 0°C between 1500 and 2100 UTC whereas it was below freezing in the simulation, which can lead to a forecast of freezing rain instead of rain. This, combined with the lack of ice pellet formation from the refreezing of partially melted ice in the simulation (Cholette et al. 2020), may explain the overestimation of freezing rain accumulation relative to the eight stations in NB shown in Fig. 7.

5. Conclusions

The ice storm that occurred on 24–26 January 2017 over the Maritime Provinces produced large amounts of precipitation, with 50 mm at Miramichi and up to 100 mm in northeastern NB reported by NB Power (Wagner 2017). The period of precipitation lasted up to 31 h. As many as 133 000 NB Power customers were without power for up to 18 days, making the storm the costliest natural disaster in NB history. Our study highlighted the meteorological factors that were responsible for the power outages using a very-high-resolution GEM simulation (1-km grid spacing). The synoptic-scale conditions associated with the storm were analyzed, and the hydrometeors formed across NB were investigated to characterize the precipitation-type transition region. The occurrence of freezing rain and near- 0°C conditions were also studied and compared with power outage data from NB Power to illustrate how adverse meteorological conditions can affect electrical transmission networks and the duration of power outages. The impact of warming from the latent heat released by the freezing of supercooled drops at the surface was investigated at four stations, three of which were coastal and one inland.

Analyses of the high-resolution simulation and field observations led to several key conclusions. These are summarized as follows:

- The slow-moving low pressure system associated with relatively strong warm-air advection aloft led to a long-duration freezing rain event over NB. The storm track may have impacted the location of the largest amounts of freezing rain.
- The persistence and extent of the melting layer aloft resulted in a large accumulation of freezing precipitation on the east coast of NB. Freezing rain was formed from both cold and warm microphysical processes (Stewart et al. 2015). As in Cholette et al. (2020), high rime mass fraction of ice aloft led to increased amounts of freezing rain at the surface, particularly near Miramichi. Freezing precipitation was produced by warm rain processes over northeastern NB and could have been mixed with wet snow to cause ice accretion.
- Considerable freezing rain accumulations were consistent with the locations of long-duration power outages. Mesoscale near-surface winds were analyzed in areas near the power distribution network. On a larger scale, transmission networks located near the coast were more affected by the storm.
- Large amounts of ice accretion associated with stronger near-surface winds and high precipitation rates led to longer power outages than in regions where precipitation rates were lower ($\sim 4 \text{ mm h}^{-1}$) but had a longer duration. Winds stronger than 25 km h^{-1} are common during freezing rain event on the coast of NB.
- The transition of precipitation types varied across eastern NB during the storm. No transitions from freezing rain to rain occurred in central and northern NB, but they were observed in southern NB. Freezing rain occurred for longer time periods in central and northern NB, leading to power outages of more than 9 days. These locations were also associated with near-surface cold-air advection that maintained conditions that were slightly below 0°C . In southern NB, warming factors such as the diurnal cycle, vertical transport, and shear-induced mixing contributed to an increase in 2-m temperatures above 0°C .
- Latent heat from the freezing of supercooled drops at the surface contributed to increasing the 2-m temperature to near 0°C , which helped locations such as Moncton (southern NB) to reach temperatures slightly $> 0^{\circ}\text{C}$ and eliminate freezing rain. The increase in temperatures to above 0°C was likely due to other factors, such as the diurnal cycle and vertical advection of warm air aloft. A cold bias in the 2-m temperature is generally obtained during freezing rain in the simulation relative to observations, which could be due to lack of warming from the release of latent heat associated with the freezing of supercooled drops at the surface.

Other factors could have impacted the duration of power outages during the storm that have not been investigated in this study. These factors include the impact of vegetation, such as tree branches falling on power lines, and the density

of the population. Southern NB, near Moncton, is more populated than the Acadian Peninsula, located in northeastern NB, where homes can be located many tens of kilometers apart. More temporal information related to the power outages and freezing rain amount would have been useful to investigate correlations with the timing of high freezing rain rates, instead of only accumulated freezing rain. Wet snow was not addressed in this study because of the limited microphysics processes available in the model, but according to NB Power (Wagner 2017), wet snow would have increased the load on the power lines in some areas. To address the occurrence of wet snow and ice pellets, further research could be conducted using the predicted liquid fraction of the ice category (Cholette et al. 2019, 2020). The relative impact of warming from latent heat released during the freezing process could be added to the land surface scheme to better address its role in the transition between precipitation types. Proximity to the ocean and sea ice cover altered the near-surface conditions during the storm. At Bas Caraquet, northerly winds persisted for a long time because of the slower moving low pressure system. The presence of sea ice would have produced lower thermal advection values, which could explain why the 2-m temperatures were colder in this area.

Understanding the meteorological factors responsible for the long-duration power outages will improve preparation for future events. The freezing rain storm that occurred over the province of NB on 24–26 January 2017 was distinct from other major freezing rain events that have affected NB Power infrastructure (Chartrand 2020), mainly because of the slower movement of the low pressure system producing persistent freezing precipitation over northeastern NB. Near-0°C conditions also played a role in the severity of winter storms. Emergency resources were not ready to deploy northward where most of the icing on electrical transmission lines occurred because freezing rain was forecast in southern locations.

Regions around the globe with sparse populations that are affected by extreme events should also be studied, even if sparse observations are available. This is important to improve weather forecasts and policy decision making but also, over the longer term, to study the impacts and adaptation required in a changing climate.

Acknowledgments. The authors acknowledge Global Water Futures funded by the Canada First Research Excellence Fund, the Canada Research Chairs Program, and the NSERC Discovery Grant program for funding this project. Author McFadden thanks Fonds de recherche du Québec—Nature et technologies (FRQNT) and NSERC for a graduate scholarship to conduct this research. Thanks are given to Katja Winger for conducting the simulations using the Global Environmental Multiscale model, version 4.8. This research was enabled in part by support from Calcul Québec (<https://www.calculquebec.ca>) and Compute Canada (<https://www.compute.canada.ca>). The authors thank Rick Fleetwood from Environment and Climate Change Canada—Atlantic Region for sharing the station data as well as Jim Samms from NB Power for contributions to this study and for sharing the power outage

duration data. The ice accumulation data were produced by Environment Canada and Climate Change Engineering Climate Services. Thanks are also given to Julien Chartrand for producing the storm tracks (Fig. 4) and providing constructive comments.

Data availability statement. The Global Environmental Multiscale (GEM) model simulations were initialized using data from ERA5, available on the date of access (<https://cds.climate.copernicus.eu/cdsapp#!/home>). Surface observations were compiled by the Environment and Climate Change Canada Atlantic Region from multiple sources and are available upon request from corresponding author Thériault. They include CoCoRaHS stations (<https://www.cocorahs.org/ViewData/>) across eastern Canada (82) and Maine (71), stations from Environment and Climate Change Canada, Nav Canada, and the Department of National Defense, as well as stations from the New Brunswick Department of Natural Resources and Energy Development (<https://www2.gnb.ca/content/gnb/en/departments/erd.html>). Data from the Historical Climate database are available on the Government of Canada website (<https://climate.weather.gc.ca>). It has been quality controlled as indicated on this website: https://climate.weather.gc.ca/climate_data/data_quality_e.html. The sounding data are from the University of Wyoming Weather Web (<http://weather.uwyo.edu>). The GEM simulations and the power outage data from NB Power are available upon request from corresponding author Thériault.

REFERENCES

- Barszcz, A., J. A. Milbrandt, and J. M. Thériault, 2018: Improving the explicit prediction of freezing rain in a kilometer-scale numerical weather prediction model. *Wea. Forecasting*, **33**, 767–782, <https://doi.org/10.1175/WAF-D-17-0136.1>.
- Bélair, S., L. Crevier, J. Mailhot, B. Bilodeau, and Y. Delage, 2003: Operational implementation of the ISBA land surface scheme in the Canadian regional weather forecast model. Part I: Warm season results. *J. Hydrometeorol.*, **4**, 352–370, [https://doi.org/10.1175/1525-7541\(2003\)4<352:OIOTIL>2.0.CO;2](https://doi.org/10.1175/1525-7541(2003)4<352:OIOTIL>2.0.CO;2).
- , J. Mailhot, C. Girard, and P. Vaillancourt, 2005: Boundary layer and shallow cumulus clouds in a medium-range forecast of a large-scale weather system. *Mon. Wea. Rev.*, **133**, 1938–1960, <https://doi.org/10.1175/MWR2958.1>.
- Benoit, R., J. Côté, and J. Mailhot, 1989: Inclusion of a TKE boundary layer parameterization in the Canadian regional finite-element model. *Mon. Wea. Rev.*, **117**, 1726–1750, [https://doi.org/10.1175/1520-0493\(1989\)117<1726:IOATBL>2.0.CO;2](https://doi.org/10.1175/1520-0493(1989)117<1726:IOATBL>2.0.CO;2).
- Best, A. C., 1949: The size distribution of raindrops. *Quart. J. Roy. Meteor. Soc.*, **75**, 16–36, <https://doi.org/10.1002/qj.49707632704>.
- Changnon, S. A., 2003: Characteristics of ice storms in the United States. *J. Appl. Meteor.*, **42**, 630–639, [https://doi.org/10.1175/1520-0450\(2003\)042<0630:COISIT>2.0.CO;2](https://doi.org/10.1175/1520-0450(2003)042<0630:COISIT>2.0.CO;2).
- Chartrand, J., 2020: Événements de pluie verglaçante ayant impacté le réseau d'énergie NB et leurs évolutions dans le futur (Freezing rain events that impacted the NB power system and their evolution in the future). Master thesis, Département des Sciences de la Terre et de l'Atmosphère, Université du Québec à Montréal., 65 pp., <https://archipel.uqam.ca/14264/1/M16926.pdf>.

- , and F. S. R. Pausata, 2020: Impacts of the North Atlantic Oscillation on winter precipitations and storm track variability in southeast Canada and the northeast United States. *Wea. Climate Dyn.*, **1**, 731–744, <https://doi.org/10.5194/wcd-1-731-2020>.
- Cheng, C. S., G. Li, and H. Auld, 2011: Possible impacts of climate change on freezing rain using downscaled future climate scenarios: Updated for eastern Canada. *Atmos.–Ocean*, **49**, 8–21, <https://doi.org/10.1080/07055900.2011.555728>.
- Cholette, M., and J. M. Thériault, 2021: Precipitation type distribution and microphysical processes during the 1998 ice storm simulated under pseudo-warmer conditions. *J. Geophys. Res. Atmos.*, **126**, e2020JD033577, <https://doi.org/10.1029/2020JD033577>.
- , H. Morrison, J. A. Milbrandt, and J. M. Thériault, 2019: Parameterization of the bulk liquid fraction on mixed-phase particles in the predicted particle properties (P3) scheme: Description and idealized simulations. *J. Atmos. Sci.*, **76**, 561–582, <https://doi.org/10.1175/JAS-D-18-0278.1>.
- , J. M. Thériault, J. A. Milbrandt, and H. Morrison, 2020: Impacts of predicting the liquid fraction of mixed-phase particles on the simulation of an extreme freezing rain event: The 1998 North American ice storm. *Mon. Wea. Rev.*, **148**, 3799–3823, <https://doi.org/10.1175/MWR-D-20-0026.1>.
- Cortinas, J. V., Jr., B. C. Bernstein, C. C. Robbins, and J. W. Strapp, 2004: An analysis of freezing rain, freezing drizzle, and ice pellets across the United States and Canada: 1976–90. *Wea. Forecasting*, **19**, 377–390, [https://doi.org/10.1175/1520-0434\(2004\)019<0377:AAOFRF>2.0.CO;2](https://doi.org/10.1175/1520-0434(2004)019<0377:AAOFRF>2.0.CO;2).
- Delage, Y., 1997: Parameterising sub-grid scale vertical transport in atmospheric models under statically stable conditions. *Bound.-Layer Meteor.*, **82**, 23–48, <https://doi.org/10.1023/A:1000132524077>.
- , and C. Girard, 1992: Stability functions correct at the free convection limit and consistent for both the surface and Ekman layers. *Bound.-Layer Meteor.*, **58**, 19–31, <https://doi.org/10.1007/BF00120749>.
- Dore, M. H. I., 2003: Forecasting the conditional probabilities of natural disasters in Canada as a guide for disaster preparedness. *Nat. Hazards*, **28**, 249–269, <https://doi.org/10.1023/A:1022978024522>.
- Girard, C., and Coauthors, 2014: Staggered vertical discretization of the Canadian Environmental Multiscale (GEM) model using a coordinate of the log-hydrostatic-pressure type. *Mon. Wea. Rev.*, **142**, 1183–1196, <https://doi.org/10.1175/MWR-D-13-00255.1>.
- Groisman, P. Ya., O. N. Bulygina, X. Yin, R. S. Vose, S. K. Gulev, I. Hanssen-Bauer, and E. Førland, 2016: Recent changes in the frequency of freezing precipitation in North America and northern Eurasia. *Environ. Res. Lett.*, **11**, 045007, <https://doi.org/10.1088/1748-9326/11/4/045007>.
- Groleau, A., A. Mailhot, and G. Talbot, 2007: Trend analysis of winter rainfall over southern Québec and New Brunswick (Canada). *Atmos.–Ocean*, **45**, 153–162, <https://doi.org/10.3137/ao.450303>.
- Gyakum, J. R., and P. J. Roebber, 2001: The 1998 ice storm—Analysis of a planetary-scale event. *Mon. Wea. Rev.*, **129**, 2983–2997, [https://doi.org/10.1175/1520-0493\(2001\)129<2983:TISA0A>2.0.CO;2](https://doi.org/10.1175/1520-0493(2001)129<2983:TISA0A>2.0.CO;2).
- Henson, W., R. E. Stewart, B. Kochtubajda, and J. M. Thériault, 2011: The 1998 ice storm: Local flow fields and linkages to precipitation. *Atmos. Res.*, **101**, 852–862, <https://doi.org/10.1016/j.atmosres.2011.05.014>.
- Hersbach, H., and Coauthors, 2020: The ERA5 global reanalysis. *Quart. J. Roy. Meteor. Soc.*, **146**, 1999–2049, <https://doi.org/10.1002/qj.3803>.
- Jeong, D., L. Sushama, M. J. F. Vieira, and K. A. Koenig, 2018: Projected changes to extreme ice loads for overhead transmission lines across Canada. *Sustainability Cities Soc.*, **39**, 639–649, <https://doi.org/10.1016/j.scs.2018.03.017>.
- Jones, K. F., 1998: A simple model for freezing rain ice loads. *Atmos. Res.*, **46**, 87–97, [https://doi.org/10.1016/S0169-8095\(97\)00053-7](https://doi.org/10.1016/S0169-8095(97)00053-7).
- Kochtubajda, B., C. Mooney, and R. E. Stewart, 2017: Characteristics, atmospheric drivers and occurrence patterns of freezing precipitation and ice pellets over the Prairie Provinces and Arctic Territories of Canada: 1964–2005. *Atmos. Res.*, **191**, 115–127, <https://doi.org/10.1016/j.atmosres.2017.03.005>.
- Kuo, H. L., 1965: On formation and intensification of tropical cyclones through latent heat release by cumulus convection. *J. Atmos. Sci.*, **22**, 40–63, [https://doi.org/10.1175/1520-0469\(1965\)022<0040:OFAIOT>2.0.CO;2](https://doi.org/10.1175/1520-0469(1965)022<0040:OFAIOT>2.0.CO;2).
- Lackmann, G. M., K. Keeter, L. G. Lee, and M. B. Ek, 2002: Model representation of freezing and melting precipitation: Implications for winter weather forecasting. *Wea. Forecasting*, **17**, 1016–1033, [https://doi.org/10.1175/1520-0434\(2003\)017<1016:MROFAM>2.0.CO;2](https://doi.org/10.1175/1520-0434(2003)017<1016:MROFAM>2.0.CO;2).
- Lamraoui, F., G. Fortin, R. Benoit, J. Perron, and C. Masson, 2013: Atmospheric icing severity: Quantification and mapping. *Atmos. Res.*, **128**, 57–75, <https://doi.org/10.1016/j.atmosres.2013.03.005>.
- Li, J., and H. W. Barker, 2005: A radiation algorithm with correlated-*k* distribution. Part I: Local thermal equilibrium. *J. Atmos. Sci.*, **62**, 286–309, <https://doi.org/10.1175/JAS-3396.1>.
- Lu, M. L., and P. Kieloch, 2005: A novel approach to the combined ice and wind. *11th Int. Workshop on Atmospheric Icing of Structures*, Montreal, QC, Canada, Quebec University and Hydro One, 95–99.
- Lu, Z., Y. Han, and Y. Liu, 2022: Occurrence of warm freezing rain: Observation and modeling study. *J. Geophys. Res. Atmos.*, **127**, e2021JD036242, <https://doi.org/10.1029/2021JD036242>.
- Makkonen, L., 1998: Modeling power line icing in freezing precipitation. *Atmos. Res.*, **46**, 131–142, [https://doi.org/10.1016/S0169-8095\(97\)00056-2](https://doi.org/10.1016/S0169-8095(97)00056-2).
- , P. Lehtonen, and M. Hirviniemi, 2014: Determining ice loads for tower structure design. *Eng. Struct.*, **74**, 229–232, <https://doi.org/10.1016/j.engstruct.2014.05.034>.
- McCray, C. D., E. H. Atallah, and J. R. Gyakum, 2019: Long-duration freezing rain events over North America: Regional climatology and thermodynamic evolution. *Wea. Forecasting*, **34**, 665–681, <https://doi.org/10.1175/WAF-D-18-0154.1>.
- , J. R. Gyakum, and E. H. Atallah, 2020: Regional thermodynamic characteristics distinguishing long- and short-duration freezing rain events over North America. *Wea. Forecasting*, **35**, 657–671, <https://doi.org/10.1175/WAF-D-19-0179.1>.
- McTaggart-Cowan, R., and Coauthors, 2019: Modernization of atmospheric physics parameterization in Canadian NWP. *J. Adv. Model. Earth Syst.*, **11**, 3593–3635, <https://doi.org/10.1029/2019MS001781>.
- Mekis, E., R. E. Stewart, J. M. Thériault, B. Kochtubajda, B. R. Bonsal, and Z. Liu, 2020: Near-0°C surface temperature and precipitation type patterns across Canada. *Hydrol. Earth Syst. Sci.*, **24**, 1741–1761, <https://doi.org/10.5194/hess-24-1741-2020>.
- Milbrandt, J. A., S. Bélair, M. Faucher, M. Vallée, M. L. Carrera, and A. Glazer, 2016: The Pan-Canadian high resolution

- (2.5 km) deterministic prediction system. *Wea. Forecasting*, **31**, 1791–1816, <https://doi.org/10.1175/WAF-D-16-0035.1>.
- Milrad, S. M., J. R. Gyakum, and E. H. Atallah, 2015: A meteorological analysis of the 2013 Alberta flood: Antecedent large-scale flow pattern and synoptic-dynamic characteristics. *Mon. Wea. Rev.*, **143**, 2817–2841, <https://doi.org/10.1175/MWR-D-14-00236.1>.
- Milton, J., and A. Bourque, 1999: A climatological account of the January 1998 ice storm in Quebec. Environment Canada Tech. Rep. CES-Q99-01, 92 pp.
- Morrison, H., and J. A. Milbrandt, 2015: Parameterization of cloud microphysics based on the prediction of the bulk ice particle properties. Part I: Scheme description and idealized tests. *J. Atmos. Sci.*, **72**, 287–311, <https://doi.org/10.1175/JAS-D-14-0065.1>.
- Panteli, M., and P. Mancarella, 2015: Influence of extreme weather and climate change on the resilience of power systems: Impacts and possible mitigation strategies. *Electr. Power Syst. Res.*, **127**, 259–270, <https://doi.org/10.1016/j.epsr.2015.06.012>.
- Pomeroy, J. W., R. E. Stewart, and P. H. Whitfield, 2016: The 2013 flood event in the South Saskatchewan and Elk River basins: Causes, assessment and damages. *Can. Water Resour. J.*, **41**, 105–117, <https://doi.org/10.1080/07011784.2015.1089190>.
- Ralph, F. M., and Coauthors, 2005: Improving short-term (0–48 h) cool-season quantitative precipitation forecasting: Recommendations from a USWRP Workshop. *Bull. Amer. Meteor. Soc.*, **86**, 1619–1632, <https://doi.org/10.1175/BAMS-86-11-1619>.
- Rannie, W., 2016: The 1997 flood event in the Red River basin: Causes, assessment and damages. *Can. Water Resour. J.*, **41**, 45–55, <https://doi.org/10.1080/07011784.2015.1004198>.
- Rauber, R. M., L. S. Olthoff, M. K. Ramamurthy, and K. E. Kunkel, 2000: The relative importance of warm rain and melting processes in freezing precipitation events. *J. Appl. Meteor.*, **39**, 1185–1195, [https://doi.org/10.1175/1520-0450\(2000\)039<1185:TRIOR>2.0.CO;2](https://doi.org/10.1175/1520-0450(2000)039<1185:TRIOR>2.0.CO;2).
- , —, —, D. Miller, and K. E. Kunkel, 2001: A synoptic weather pattern and sounding-based climatology of freezing precipitation in the United States east of the Rocky Mountains. *J. Appl. Meteor.*, **40**, 1724–1747, [https://doi.org/10.1175/1520-0450\(2001\)040<1724:ASWPAS>2.0.CO;2](https://doi.org/10.1175/1520-0450(2001)040<1724:ASWPAS>2.0.CO;2).
- Ressler, G. M., S. M. Milrad, and E. H. Atallah, 2012: Synoptic-scale analysis of freezing rain events in Montreal, Quebec, Canada. *Wea. Forecasting*, **27**, 362–378, <https://doi.org/10.1175/WAF-D-11-00071.1>.
- Rezaei, S. N., L. Chouinard, S. Langlois, and F. Légeron, 2016: Analysis of the effect of climate change on the reliability of overhead transmission lines. *Sustainability Cities Soc.*, **27**, 137–144, <https://doi.org/10.1016/j.scs.2016.01.007>.
- Roebber, P. J., and J. R. Gyakum, 2003: Orographic influences on the mesoscale structure of the 1998 ice storm. *Mon. Wea. Rev.*, **131**, 27–50, [https://doi.org/10.1175/1520-0493\(2003\)131<0027:OIOTMS>2.0.CO;2](https://doi.org/10.1175/1520-0493(2003)131<0027:OIOTMS>2.0.CO;2).
- Ryerson, C. C., and A. C. Ramsay, 2007: Quantitative ice accretion information from the automated surface observing system. *J. Appl. Meteor. Climatol.*, **46**, 1423–1437, <https://doi.org/10.1175/JAM2535.1>.
- Stewart, R. E., 1991: Canadian Atlantic storms program: Progress and plans of the meteorological component. *Bull. Amer. Meteor. Soc.*, **72**, 364–371, [https://doi.org/10.1175/1520-0477\(1991\)072<0364:CASPPA>2.0.CO;2](https://doi.org/10.1175/1520-0477(1991)072<0364:CASPPA>2.0.CO;2).
- , J. M. Thériault, and W. Henson, 2015: On the characteristics of and processes producing winter precipitation types near 0°C. *Bull. Amer. Meteor. Soc.*, **96**, 623–639, <https://doi.org/10.1175/BAMS-D-14-00032.1>.
- Stuart, R. A., and G. A. Isaac, 1999: Freezing precipitation in Canada. *Atmos.–Ocean*, **37**, 87–102, <https://doi.org/10.1080/07055900.1999.9649622>.
- Szeto, K. K., A. Tremblay, H. Guan, D. R. Hudak, R. E. Stewart, and Z. Cao, 1999: The mesoscale dynamics of freezing rain storms over eastern Canada. *J. Atmos. Sci.*, **56**, 1261–1281, [https://doi.org/10.1175/1520-0469\(1999\)056<1261:TMDOFR>2.0.CO;2](https://doi.org/10.1175/1520-0469(1999)056<1261:TMDOFR>2.0.CO;2).
- Thériault, J. M., R. E. Stewart, J. A. Milbrandt, and M. J. Yau, 2006: On the simulation of winter precipitation types. *J. Geophys. Res.*, **111**, D18202, <https://doi.org/10.1029/2005JD006665>.
- Wagner, J., 2017: Analyse de la tempête de verglas 2017 Nouveau-Brunswick (Analysis of the 2017 New Brunswick ice storm). Government of New Brunswick Rep., 185 pp., https://www2.gnb.ca/content/dam/gnb/Departments/eco-bce/Promo/ice_storm_meetings/PDFs/ice_storm_review-f.pdf.
- Yip, T.-C., 1995: Estimating icing amounts caused by freezing precipitation in Canada. *Atmos. Res.*, **36**, 221–232, [https://doi.org/10.1016/0169-8095\(94\)00037-E](https://doi.org/10.1016/0169-8095(94)00037-E).
- Zerr, R. J., 1997: Freezing rain: An observational and theoretical study. *J. Appl. Meteor.*, **36**, 1647–1661, [https://doi.org/10.1175/1520-0450\(1997\)036<1647:FRAOAT>2.0.CO;2](https://doi.org/10.1175/1520-0450(1997)036<1647:FRAOAT>2.0.CO;2).